RESEARCH ARTICLE
doi: 10.2306/scienceasia1513-1874.2026.015

ScienceAsia 52 (1): 2026: ID 2026015: **1–8**

Enzymatic hydrolyses of glucurono(arabino)xylan from two pasture crops, purple guinea (*Panicum maximum* TD58) and Napier (*Pennisetum purpureum* × *Pennisetum americanum*) grasses

Sorawit Na Nongkhai[a,b,c], **Wichanee Bankeeree**[b], **Hunsa Punnapayak**[b], **Sehanat Prasongsuk**[b], **Pongtharin Lotrakul**[b,*]

[a] Program in Biotechnology, Faculty of Science, Chulalongkorn University, Bangkok 10330 Thailand
[b] Plant Biomass Utilization Research Unit, Department of Botany, Faculty of Science, Chulalongkorn University, Bangkok 10330 Thailand
[c] Department of Biochemistry, Faculty of Medicine, Bangkokthonburi University, Bangkok 10170 Thailand

*Corresponding author, e-mail: pongtharin.l@chula.ac.th

Received 3 Mar 2025, Accepted 27 Jan 2026
Available online

ABSTRACT: In this study, purple guinea grass (PG) and Napier grass (NG) were demonstrated and validated as great sources of xylan and, after enzymatic hydrolysis, xylooligosaccharides (XOs) and xylose. A simple alkaline extraction gave near-complete recoveries of xylan from both plants. Based on Response Surface Methodology, the highest xylan yields from PG (95.9 ± 7.6% recovery) and NG (93.5 ± 3.9% recovery) were obtained, respectively, under the following condition: 13.3% (w/v) NaOH, a liquid-to-solid ratio of 13.3:1, 121 °C/15 psi, and 44 min; 16.8% (w/v) NaOH, a liquid-to-solid ratio of 14.75:1, 121 °C/15 psi, and 30 min. Analyses of sugar composition and FTIR spectra confirmed that xylan from both PG and NG was glucurono(arabino)xylan. These xylans were partially hydrolyzed to obtain XOs using crude endoxylanase while completely hydrolyzed to obtain xylose using a mixture of crude endoxylanase and β-xylosidase, both from *Aureobasidium pullulans*. After optimization, the highest yields of both XOs and xylose from PG were significantly enhanced. The yields of reducing sugars (170.3 ± 10.3 mg/g xylan) and combined xylobiose and xylotriose (121.2 ± 1.9 mg/g xylan) were maximized at 74.9 U/g xylan of endoxylanase after 64-h incubation. For xylose, the yield (179.4 ± 3.2 mg/g xylan) was highest at 69.9 U/g xylan and 70.0 U/g xylan of endoxylanase and β-xylosidase, respectively, after 18-h incubation. Slightly lower yields of reducing sugars (166.4 ± 4.3 mg/g xylan), combined xylobiose and xylotriose (112.2 ± 1.8 mg/g xylan), and xylose (138.8 ± 3.8 mg/g xylan) were obtained from NG.

KEYWORDS: xylooligosaccharides, xylose, Napier grass xylan, purple guinea grass xylan

INTRODUCTION

Hemicellulose, the second most abundant polysaccharide in plant cell wall, has attracted considerable interest due to various industrial applications including biomedicine, food packaging, and novel materials [1]. Plant biomasses, especially those from agricultural wastes and fast-growing crops, have received much interest as the sources of hemicellulose [2, 3]. Many perennial grasses, including Napier grass (NG) (*Pennisetum purpureum* x *Pennisetum americanum*) and purple guinea grass (PG) (*Panicum maximum*) which are forage crops commonly used as animal feeds [2, 4], exhibit relatively rapid biomass production [4]. The rapid growth of these pasture crops makes them attractive as potential sources of lignocellulosic biomasses for the manufacturing of value-added compounds [2]. Most studies have emphasized the applications of NG and PG celluloses for film synthesis [5] and biofuel production including production of butanol [6] and ethanol [7]. On the contrary, only a few reports have focused on the utilization of NG and PG hemicelluloses, especially in saccharification for xylooligosaccharides (XOs) [8] and xylose [9], despite the fact that these grass biomasses contain significant amount of it.

After cellulose, hemicellulose is the second most plentiful polysaccharide of which the major component is xylan. It can be digested, through acid and enzymatic hydrolyses, and transformed into value-added products, including XOs and xylose. In acid hydrolysis, it is non-specific and can generate undesirable byproducts, such as furfural, and high amounts of unwanted monosaccharides which require a purification step in the downstream process. Therefore, enzymatic hydrolysis is considered as a more feasible method with high specificity and product quality [10]. XOs are xylose oligomers that can be applied as supplements for food and pharmaceutical products because of their prebiotic property. They can be produced through partial enzymatic hydrolysis using endoxylanase [11]. Regarding xylose, it is commonly used as the substrate for fermented products, including xylitol, isobutanol, lactic acid or lipids. Xylose can be produced through complete enzymatic hydrolysis using endoxylanase and

β-xylosidase [12]. Both enzymes can be produced by several bacteria and fungi, including the cosmopolitan, polymorphic ascomycetous *Aureobasidium pullulans*, commonly known as black yeasts. It has been reported that *A. pullulans* is an excellent xylanolytic enzyme producer. Many xylanase-overproducing color-variant strains have been isolated in Thailand, and their enzymes have revealed encouraging prospects in industrial applications [13]. Therefore, it is of interest to investigate the potential of PG and NG as the sources of xylan and in subsequent XOs and xylose production via enzymatic hydrolyses using crude *A. pullulans* endoxylanase and β-xylosidase under the optimal conditions determined by response surface methodology (RSM). RSM has been widely used in many optimization studies since it provides advantages over the conventional one-factor-at-a-time design, especially the ability to estimate interactions among variables and the significant reduction in experimental time and resources [14]. The development of large-scale saccharification can be further expanded from these results, which would increase the value of both PG and NG to that of more than just cheap animal feeds.

This study illustrates the prospect of PG and NG as the significant source of xylan since they are fast-growing and readily available. The nearly complete xylan recoveries obtained from both grasses through simple NaOH extraction make them attractive as the substrates for industrial xylan production. The obtained xylans are shown to be readily digestible by xylan-hydrolyzing enzymes and yield valuable products such as XOs and xylose that can be further explored for their potential in food and pharmaceutical industries.

MATERIALS AND METHODS

Microorganisms and grass samples

NG and PG (breeding line TD58) used in this study were parts of the cultivar collections used in breeding programs and were grown and harvested at Nakhon Ratchasima Animal Nutrition Research and Development Center, Nakhon Ratchasima Province, and Phetchaburi Animal Nutrition Research and Development Center, Phetchaburi Province, Thailand, respectively. Grass samples were cut, dried in an oven at 60 °C until consistent weights were achieved, and then stored in plastic bags. For the xylanolytic enzyme production, *A. pullulans* NRRL 58523 and CBS 135684 were obtained from the culture collection of the Plant Biomass Utilization Research Unit, Department of Botany, Faculty of Science, Chulalongkorn University, Bangkok, Thailand [13, 15]. For long-term storage, the yeasts were cultured in yeast malt (YM) broth at room temperature (28 ± 2 °C) with agitation (150-rpm) for 3 days and kept at −20 °C after being lyophilized in 15% (w/v) skim milk. For ongoing experiments, the yeasts were maintained on YM agar and stored in a refrigerator (10 ± 2 °C).

Biomass composition, xylan extraction and optimization

Cellulose, hemicellulose, and lignin contents in NG and PG were determined as described [8]. For preliminary extraction, NG xylan (NGX) and PG xylan (PGX) were extracted by 12% (w/v) NaOH with a liquid-to-solid ratio of 10:1 in an autoclave (121 °C, 15 psi) for 45 min [2]. Xylan yield and relative xylan recovery were calculated by Eqs (1) and (2):

$$\text{Xylan yield (\%)} = \frac{\text{Dry weight of the extracted xylan (g)}}{\text{Dry weight of the grass sample (g)}} \times 100 \quad (1)$$

$$\text{Relative xylan recovery (\%)} = \frac{\text{Xylan yield (\%)}}{\text{Total hemicellulose content (\%)}} \times 100 \quad (2)$$

In order to optimize the xylan extraction, three variables were included in Box-Behnken design (BBD) [16]: NaOH concentrations (12, 15, 18% (w/v)), steaming times (30, 45, 60 min in an autoclave at 121 °C and 15 psi), and liquid-to-solid ratios (5:1, 10:1, 15:1 ml/g). Design Expert, version 7.0 (Stat-Ease Inc., USA) was used for RSM analysis in order to forecast the optimal condition that gave the maximum relative xylan recovery. An independent experiment was then conducted to confirm the predicted conditions, and Student's *t*-test was used to compare the values (SPSS statistical computer package version 16, SPSS Inc., USA).

Sugar composition and structural analyses

NGX, PGX and the commercial beechwood xylan (Megazyme, Ireland) as the reference were hydrolyzed by 4% (v/v) H_2SO_4 with a liquid-to-solid ratio of 10:1 (10 ml/g) in an autoclave for 1 h [17]. Then, hydrolysates were neutralized by Ca_2CO_3 and the sugar content was quantified by high performance liquid chromatography (HPLC) using a refractive index detector (Shimadzu, Japan) and a Shodex Asahipak NH2P-50 4E column at 40 °C with 5 mM H_2SO_4 as the mobile phase at a flow rate of 0.6 ml/min. Analytical graded xylose, glucose, arabinose, galacturonic acid and glucuronic acid were used as standards (Sigma-Aldrich, USA) [17]. For the xylan structural analysis, Fourier-transform infrared (FTIR) spectroscopy in the 4000–400 cm^{-1} region using a KBr disc containing 1% (w/w) of the ground xylan sample at a ratio of 10:1 (by weight) was used according to previous study [17].

Production of xylanolytic enzymes

Aureobasidium pullulans NRRL 58523 and CBS 135684 were used for the endoxylanase and β-xylosidase production, respectively. Both enzymes were selected based on their high activity and thermostability at 50 °C

[13, 15, 16]. For seed culture preparation, both strains were cultivated in YM broth at room temperature (28 ± 2 °C) with 150-rpm agitation for 3 days. Each seed culture was transferred to a 0.1% (v/v) endoxylanase/ β-xylosidase production medium containing ground corncob (1% w/v) as the sole carbon source according to previous study [18]. The cultures were incubated at room temperature with 150-rpm agitation for 3 days. The NRRL 58523 culture supernatant was collected by centrifugation (6,000 × *g*, 10 min) and used as the crude endoxylanase [18]. After centrifugation under the same conditions, the CBS 135684 cell pellet was collected, washed several times with deionized water, then manually ground into a fine powder in liquid nitrogen. After being suspended in a small volume of deionized water, the cell lysate was centrifuged, and the supernatant was used as the crude β-xylosidase [15].

The endoxylanase activity was measured using commercial beechwood xylan (Megazyme) as the substrate [16] and the released reducing sugars were quantified by using 3,5-dinitrosalicylic acid (DNS) according to the method described [19]. For the β-xylosidase assay, the enzyme activity was determined using *p*-nitrophenyl-β-D-xylopyranoside (*p*NPX) as the substrate. The reaction mixtures containing 10 µl 2.5 mM *p*NPX, 25 µl enzyme solution, 65 µl distilled water, and 100 µl 100 mM sodium citrate buffer (pH 4) were incubated in a water bath at 70 °C for 10 min. Then, 200 µl of 0.1 M Na_2CO_3 was added to stop the reaction and the absorbance was measured at 405 nm. The *p*-nitrophenol standard curve was used for activity calculation [15]. The amount of enzyme that catalyzes the release of one µmole xylose/*p*-nitrophenol equivalent per min was defined as one unit (U) of xylanase/ β-xylosidase [15, 16].

Enzymatic hydrolyses and optimization

For the partial enzymatic hydrolysis for XOs production, the reaction mixture (10 ml in a 20 ml Erlenmeyer flask) containing the xylan substrate (1% (w/v)) and the crude endoxylanase (50 U/g xylan) in 50 mM sodium citrate buffer (pH 4) was incubated with 150-rpm agitation at the optimal temperature (50 °C) for 24 h [16]. After hydrolysis, the mixture was heated at 100 °C for 10 min to denature the enzyme [8], and the released reducing sugars were quantified as described [16, 19]. To optimize the partial hydrolysis, the xylanase dosage (25, 50, 75 U/g xylan) and incubation time (24, 48, 72 h) were subjected to the central composite design (CCD) and RSM to predict the conditions that would give the maximal yield of reducing sugars. The content of xylobiose (X2) and xylotriose (X3) in the hydrolysate was measured by HPLC (Shimadzu) using refractive index detector and Shodex sugar sp0810 column (Showa Denko, Japan) at 40 °C with 5 mM H_2SO_4 as mobile phase at a flow rate 0.6 ml/min to compare with standard sugars including xylose (Sigma-aldrich), xylobiose and xylotriose (Megazyme). The validation of the predicted conditions was conducted in an independent experiment with three replicates, and the results were compared using Student's *t*-test.

For xylose production, the complete enzymatic hydrolysis was conducted in 20 ml Erlenmeyer flasks with the reaction mixtures (10 ml) containing 1% (w/v) xylan in 50 mM sodium citrate buffer (pH 4) and the combined crude enzymes (50 U/g xylan for each enzyme). The reaction mixtures were incubated at 50 °C with 150-rpm agitation for 12 h. The reaction was stopped by boiling at 100 °C for 10 min [20, 21], and the xylose content in the hydrolysates was detected by HPLC. To improve the xylose yield, BBD and RSM were applied with various endoxylanase dosages (30, 50, 70 U/g xylan), β-xylosidase dosages (30, 50, 70 U/g) and incubation times (6, 12, 18 h). The validation of the predicted condition was carried out as described above.

Statistical analysis

The experiments were carried out in three replicates and the results were presented as mean values with one standard deviation. The experimental data were analyzed using one-way ANOVA with Duncan's multiple range test (DMRT), or Student's *t*-test when appropriate (SPSS statistical computer package version 16, SPSS Inc.). Significant difference was determined at $p < 0.05$.

RESULTS AND DISCUSSION

Biomass composition

Both NG and PG biomass compositions were similar. They comprised about 31.3–33.8% (w/w) cellulose, 27.7–33.7% (w/w) hemicellulose, 6.0–8.7% (w/w) lignin, 2.7–3.0% (w/w) ash, and 23.3–29.7% (w/w) others (Table S1). These two grasses showed high potential as the sources of xylan due to their low lignin content compared to other grass crops (about 4–20% (w/w)), including vetiver grass [8], *Sehima* grass [2], cogon grass [8], Pangola grass, ruzi grass, and *Miscanthus* grass [4]. Moreover, both NG and PG have been found to be available year round on a large scale, especially in sub-tropical and tropical areas [4], which is attractive in terms of feedstock availability, logistic practices, and transportation cost. Although biomass availability has also been reported in other pasture grass crops, including vetiver grass (9 ton/ha/year [4]), para grass (10 ton/ha/year [22]), and switchgrass (3 ton/ha/year [23]), both NG and PG have been found to be far more productive at 51–87 ton/ha/year [4, 24] and 15–19 ton/ha/year [4], respectively.

Alkali extraction and optimization

Xylan can be extracted by using different methods such as alkaline extraction or acid extraction. However, NaOH is more widely used due to the higher solubility of the obtained xylan and the greater degree of enzymatic hydrolysis. Moreover, unlike acid extraction, NaOH extraction does not produce harmful byproducts, such as furfural, which inhibit the subsequent microbial activity [2]. In preliminary hydrolysis, the relative xylan recovery values of NGX and PGX were 68.6 ± 0.9% and 76.8 ± 3.2%, respectively. To improve the extraction efficiency, three levels of three variable factors which were previously found to affect the xylan yield from sugarcane leaf [16] were selected for investigation using a Box-Behnken design in this study (Table S2). ANOVA was employed to analyze the statistical significance of the models (Table S3 and Table S4), and the data based on a second-order polynomial was expressed by Eqs (3) and (4) as follows.

$$Y_1 = 20.15X_1+1.80X_2+125.26X_3-0.08X_1X_2+1.07X_1X_3 - 0.14X_2X_3-0.60X_1^2-0.01X_2^2-24.23X_3^2-286.69 \quad (3)$$

$$Y_2 = 11.07X_1+2.27X_2+174.52X_3-0.01X_1X_2-1.87X_1X_3 - 0.17X_2X_3-0.17X_1^2-0.02X_2^2-26.89X_3^2-264.79 \quad (4)$$

where Y_1 and Y_2 were the relative xylan recovery (% w/w) of NGX and PGX, respectively, X_1 was the NaOH concentration (% w/v), X_2 was the steaming time (min) and X_3 was the liquid-to-solid ratio (ml/g). According to ANOVA analysis of NGX extraction, 99% of the observed response could be explained by the equation ($R^2 = 0.99$). The regression model was significant ($p = 0.0001$) whereas lack of fit was not significant ($p = 0.30$) which indicated that it could accurately predict the response. Moreover, the coefficient of variation (CV) at 3.7% indicated the reliability and precision of the experiments. ANOVA analysis also reveals that the relative xylan recovery from NG is subject to significant interaction effects among the tested factors. Specifically, the recovery is significantly influenced by the interaction between NaOH concentration (X_1) and steaming time (X_2), and the interaction between NaOH concentration (X_1) and liquid-to-solid ratio (X_3). These significant interactions indicate that the optimal setting for X_1 (NaOH concentration) depends on the level chosen for X_2 or X_3. Conversely, the effect of steaming time (X_2) is independent of the liquid-to-solid ratio (X_3), suggesting their combined influence on the yield is primarily additive rather than synergistic or antagonistic. The RSM predicted that using a 14.75:1 liquid-to-solid ratio and 16.8% (w/v) NaOH for 30 min yielded the highest relative xylan recovery (96.9%) as shown in the response surface plots (Fig. S1). NGX was extracted following the recommended conditions to confirm the prediction. The result showed that the relative xylan recovery of 93.5 ± 3.9% was not significantly different from the predicted value ($p = 0.25$), suggesting that the equation was accurate. Using these optimized conditions, the amount of xylan extracted from NG was 1.36-fold higher than that using the preliminary conditions (68.6 ± 0.9%).

For optimization of PGX extraction, 96% of the observed response could be determined by the equation ($R^2 = 0.96$). Despite the relatively high CV (12.2%), the model's significance ($p = 0.0044$) and insignificance of lack of fit ($p = 0.06$) indicated that the regression model could predict the responses accurately. The RSM predicted that the highest relative xylan recovery (99.9%) could be reached when the extraction was carried out in 13.3% (w/v) NaOH in an autoclave for 44 min with a liquid-to-solid ratio of 13.3:1 as shown in the contour plots (Fig. S2). A relative xylan recovery of 95.9 ± 7.6% under the recommended conditions was obtained, and it was not significantly different from the predicted value ($p = 0.58$). Using these optimized conditions, the PGX recovery value (95.9 ± 7.6%) was 1.25-fold higher than that using the preliminary conditions (76.8 ± 3.2%). In this study, the near complete xylan recovery (>93%) from both grasses, which was achieved after optimization, was higher than that of the previous reports on xylan extraction from NG (67 to 86%) [8, 25, 26]. Interestingly, no attempt on PGX extraction has been reported. Moreover, the optimal conditions in this study did not require an excessive NaOH concentration and long extraction period, unlike those of previous reports on other grasses including 8–12% (w/v) NaOH concentrations, 45–480 min incubation times and liquid-to-solid ratio of 10–25:1, with relative xylan recovery percentages between 61 and 89% [2, 27, 28].

Sugar composition and structural analyses

Structures of NGX and PGX were determined by using their FT-IR spectra and comparing them with the spectra of commercial beechwood xylan. The spectra pattern of all samples are shown in Fig. 1. All three xylans showed peaks at 3437, 2920, 1415, 1407, 1046, 897, 639 and 530 cm^{-1}, which were typical of xylans. The stretching of the H-bond in the OH group and C—H stretching were visible in the NGX and PGX spectra at 3437 and 2920 cm^{-1}, respectively [29]. The peak appearance at 1415 cm^{-1} revealed the carboxyl group stretching of the glucuronic acid [30]. The peak at 1407 cm^{-1} was C—H stretching, whereas the C—O, C—C, and C—OH bending of the xylose pyran ring were observed at 1046 cm^{-1} [29]. The spectra band at 897 cm^{-1} correlated to the stretching vibration in C—O—C, which indicated the β-1,4-xylosidic linkage of the xylan structure [29]. Moreover, the peaks at 639 and 530 cm^{-1} expressed the stretching or bending of C—C—H or C—O—C [29]. The appearance of obtained NGX and PGX peaks at 989 cm^{-1} was due to the presence of an arabinose side chain [31] and the

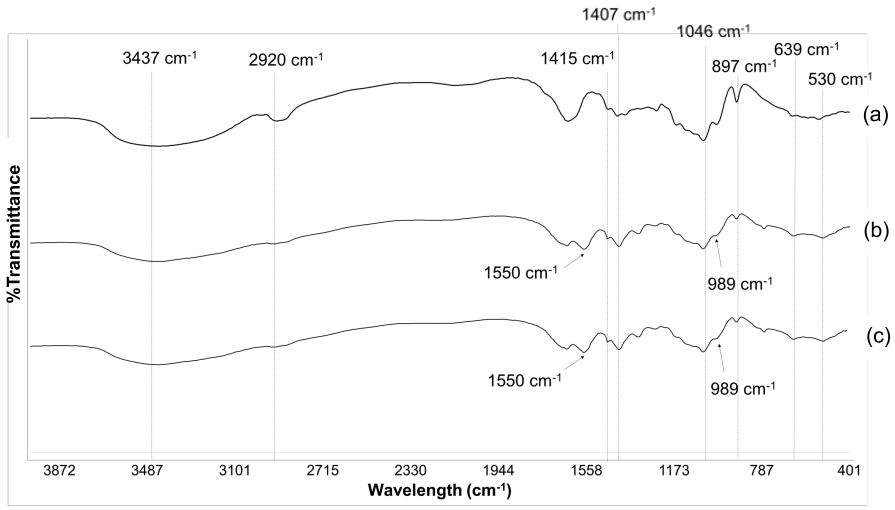

Fig. 1 The FT-IR spectra pattern of xylan: (a) commercial beechwood xylan, (b) NGX, and (c) PGX.

peak at 1550 cm^{-1} originated from the phenolic ring absorbance of lignin [2].

Regarding the sugar analysis (Table S5), xylose (76.7 and 77.2%, respectively) was detected as the dominant sugar component in NGX and PGX. Smaller amounts of arabinose (20.6 and 20.9%, respectively) and trace amounts of glucuronic acid (2.2 and 2.4%, respectively) were observed indicating that both xylans were glucurono(arabino)xylans. The glucurono(arabino)xylans from NG and PG were similar in structure to those from switchgrass [32], Chinese silver grass [33], and stiff brome grass [34].

Partial enzymatic saccharification

Based on the preliminary experiment, the amounts of reducing sugars, which were 140.1 ± 0.0 and 153.2 ± 5.0 mg/g xylan, were obtained from the partial hydrolyses of NGX and PGX, respectively, by using the crude *A. pullulans* NRRL 58523 endoxylanase (50 U/g xylan) in 50 mM sodium citrate buffer (pH 4.0) and incubating it at 50 °C for 24 h. Using five levels of two variable factors, the CCD was employed to optimize the production of XOs from both xylans. The response values (amounts of reducing sugars) with predicted values are presented in Table S6. The statistical significance of both models was determined by ANOVA (Table S7 and Table S8), and the second-order polynomials equations (Eqs (5) and (6)) were derived from the actual data as follows:

$$R_{NGX} = 2.79A_1 + 1.85A_2 + 0.01A_1A_2 - 0.02A_1^2 - 0.01A_2^2 + 4.86 \quad (5)$$

$$R_{PGX} = 3.03A_1 + 2.10A_2 + 0.01A_1A_2 - 0.02A_1^2 - 0.01A_2^2 - 8.99 \quad (6)$$

where R_{NGX} and R_{PGX} were the amounts of reducing sugars (mg/g xylan obtained from NG and PG, respectively), A_1 was the endoxylanase dosage (U/g xylan) and A_2 was the incubation time (h). Based on the ANOVA statistical significance model (Table S7 and Table S8), the equations from both models exhibited R^2 values of 0.96 and 0.99, respectively. The models for NGX and PGX hydrolyses were significant, with $p < 0.0013$ and $p < 0.0001$, respectively, whereas lack of fit was not significant ($p < 0.26$ and $p < 0.17$, respectively), indicating that the regression models could accurately predict the responses. Moreover, the low CVs (< 4.1% and < 0.9%, respectively) indicated that the experiments were precise and reliable. The response surface plots from both models are shown in Fig. S3. To improve XOs production from NGX, the RSM was used to predict that the maximum amount of reducing sugars (168.8 mg/g xylan) could be achieved when endoxylanase was used at a dosage of 74.9 U/g xylan and the mixture was incubated for 64 h. For PGX, the RSM predicted that the maximum amount of reducing sugars (172.1 mg/g xylan) could be obtained when endoxylanase was used at a dosage of 74.9 U/g xylan with an incubation time of 64 h. In independent validation experiments, reducing sugar amounts of 166.4 ± 4.3 and 170.3 ± 10.3 mg/g xylan were obtained from NGX ($p = 0.49$) and PGX ($p = 0.78$), respectively, which were not significantly different from the predicted values, indicating that the equations were accurate. Using these optimized conditions, the amounts of reducing sugars obtained from NGX and PGX were 1.19- and 1.11-fold higher than those obtained using preliminary conditions, respectively. In addition, XOs yields, including combined X2 and X3 obtained from NGX and PGX under these optimized conditions, were 112.2 ± 1.8 and 121.2 ± 1.9 mg/g xylan, respectively. Mass balances for XOs production

from both xylans were 35.3 and 32.2 mg/g biomass, respectively (Fig. S4 and Fig. S5).

Although previous reports showed that acid hydrolysis provided higher XOs yields than the enzymatic hydrolysis method, enzymatic hydrolysis yielded more X2 and X3 than acid hydrolysis [10]. X2 and X3 have reportedly shown higher market values than XOs with a higher degree of polymerization. Moreover, they are sold as functional food products with higher prebiotic properties [35]. In this study, XOs yields of 11 and 12% were obtained from NGX and PGX, respectively, when digested with 75 U/g xylan endoxylanase for 64 h. This was similar to other previous reports, in which slightly lower XOs yields were obtained from *Sehima* grass (11%) [2], NG (7%) [8], and vetiver grass (9%) [8] by using xylanase dosages from 10 to 70 U/g xylan and incubation times from 17 to 96 h.

Complete enzymatic hydrolysis

Complete xylan hydrolysis was carried out by using a combination of endoxylanase and β-xylosidase in a simultaneous digestion or one-step process. This synergy of both enzymes has been reported to efficiently improve the hydrolytic yield. Moreover, simultaneous digestion has been shown to enhance enzymatic conversion speed and cost-effectiveness due to reduction of enzyme loading and incubation time [36]. According to the preliminary experiments (50 U/g xylan endoxylanase and 50 U/g xylan β-xylosidase at 50 °C for 12 h) (data not shown), xylose yields of 128.9 ± 1.5 and 132.4 ± 0.8 mg/g xylan were obtained from NGX and PGX, respectively. To enhance the xylose yield of both xylans, BBD was designed with three levels of three variable factors, and the response values are showed in Table S9. The statistical significance of the models was calculated by ANOVA (Table S10 and Table S11), and the data based on a second-order polynomial was expressed by Eqs (7) and (8) as follows.

$$XY_{NGX} = 0.29B_1 + 0.74B_2 + 8.10B_3 - 0.002B_1B_2 - 0.02B_1B_3 - 0.03B_2B_3 + 0.004B_1^2 - 0.001B_2^2 - 0.16B_3^2 + 27.50 \quad (7)$$

$$XY_{PGX} = 176.9 - 4.05B_1 - 0.68B_2 + 5.89B_3 + 0.01B_1B_2 + 0.02B_1B_3 - 0.01B_2B_3 + 0.04B_1^2 + 0.01B_2^2 - 0.16B_3^2 \quad (8)$$

where XY_{NGX} and XY_{PGX} were the xylose yields (mg/g xylan) obtained from NGX and PGX, respectively, B_1 was the endoxylanase dosage (U/g xylan), B_2 was the β-xylosidase dosage (U/g xylan), and B_3 was the incubation time (h). Based on ANOVA analysis of enhancement of xylose production from NGX (Table S10), the equation exhibited an R^2 value of 0.98. The regression model could accurately predict the response, as evidenced by the significant model ($p = 0.0010$) and non-significant lack of fit ($p = 0.31$). Moreover, the experiments' accuracy and reliability were demonstrated by their low CV (2.2%). The RSM assessment (Fig. S6) showed that the optimum conditions could be achieved when adjusting the xylan endoxylanase dosage to 68.1 U/g, the xylan β-xylosidase dosage to 63.1 U/g and the incubation time to 17 h, resulting in a xylose yield of 143.6 mg/g xylan. Complete hydrolysis of NGX was performed under the suggested conditions to confirm the prediction, and it showed that the xylose yield of 138.8 ± 3.8 mg/g xylan was not significantly different ($p = 0.16$), indicating that the equations were accurate. Under optimized conditions, the xylose yield was slightly higher than the yield obtained using the preliminary conditions.

Regarding the improvement of xylose production from PGX, according to the ANOVA statistical significance model (Table S11), the equation exhibited an R^2 value of 0.91. The model was significant, with $p = 0.03$, whereas lack of fit was not significant ($p = 0.06$), in addition, the low coefficient of variation (CV = 6.3%) indicated the high accuracy, precision, and reliability of the experiments. The contour plots are shown in Fig. S7. The RSM assessment showed that the maximum xylose yield (181.9 mg/g xylan) could be received when endoxylanase and β-xylosidase were used in dosages of 69.9 U/g xylan and 70.0 U/g xylan, respectively, with an 18-h incubation time. An independent experiment performed under the suggested conditions gave the maximum xylose yield of 179.4 ± 3.2 mg/g xylan, which was not significantly different from the predicted value ($p = 0.65$). Using these optimized conditions, the xylose yield from PGX was 1.35-fold higher than obtained using the preliminary conditions. The mass balances for xylose production from NGX and PGX were 43.7 and 47.6 mg/g biomass, respectively (Fig. S4 and Fig. S5).

Most previous studies on complete hydrolysis of grass xylans were conducted by using acid hydrolysis treatment, which yielded higher amounts of xylose monomer [9]. However, the enzymatic hydrolysis method in this study did not produce undesirable toxic byproducts, such as furfural (Fig. S8), which could inhibit subsequent microbial activities, including fermentation and biotransformation [37]. The complete xylan hydrolysis after optimization in this study yielded xylose from NGX (14%) and PGX (18%) with a 68–70 U/g xylan endoxylanase dosage and a 63–70 U/g xylan β-xylosidase dosage, respectively, after incubation for 18 h. They exhibited xylose yields similar to those of previous reports on other agricultural residues (between 13 and 16%) with hydrolysis conditions of 8–500 U/g xylan endoxylanase dosages and 8–100 U/g xylan β-xylosidase dosages, and incubation for 72 h [38, 39].

CONCLUSION

NG and PG were shown to have high potential as sources of xylan for XOs and xylose production. The extraction efficiency for both NGX and PGX improved

significantly, with nearly complete xylan recovery ($93.5 \pm 3.9\%$ and $95.9 \pm 7.6\%$ recovery, respectively). Conditions for partial and complete enzymatic hydrolysis were also optimized, with a significant improvement in XOs yield for NGX (112.2 ± 1.8 mg/g xylan), and both XOs and xylose yields for PGX (121.2 ± 1.9 mg/g xylan and 179.4 ± 3.2 mg/g xylan, respectively). The hydrolyzed products were also free of furfural which make them suitable for further studies on their prospects in food and pharmaceutical applications such as prebiotics and xylitol productions. Considering the much higher number of studies focusing on the yield of NGX than that of PGX, it is important to note that PG was shown to be a comparable source of xylan, XOs and xylose to NG, if not better.

Appendix A. Supplementary data

Supplementary data associated with this article can be found at https://dx.doi.org/10.2306/scienceasia1513-1874.2026.015.

Acknowledgements: This research was funded by the 100th Anniversary Chulalongkorn University Fund for Doctoral Scholarship, the 90th Anniversary of Chulalongkorn University Fund (Ratchadaphiseksomphot Endowment Fund) and The Overseas Research Experience Scholarship for Graduate Student from Graduate School, Chulalongkorn University. Moreover, authors are thankful to their respective departments and university for providing facilities. Suggestions from Professor Witoon Prinyawiwatkul are deeply appreciated.

REFERENCES

1. He Y, Liu Y, Zhang M (2024) Hemicellulose and unlocking potential for sustainable applications in biomedical, packaging, and material sciences: A narrative review. *Int J Biol Macromol* **280**, 135657.
2. Samanta AK, Jayapal N, Kolte AP, Senani S, Sridhar M, Suresh KP, Sampath KT (2012) Enzymatic production of xylooligosaccharides from alkali solubilized xylan of natural grass (*Sehima nervosum*). *Bioresour Technol* **112**, 199–205.
3. Sophonputtanaphoca S, Prasongsuk S, Chutong P, Samathayanon C, Cha-Aim K (2023) Utilization of sugarcane bagasse for synthesis of carboxymethylcellulose and its biodegradable blend films. *ScienceAsia* **49**, 541–552.
4. Banka A, Komolwanich T, Wongkasemjit S (2014) Potential Thai grasses for bioethanol production. *Cellulose* **22**, 9–29.
5. Indira Devi MP, Nallamuthu N, Rajini N, Varada Rajulu A, Hari Ram N, Siengchin S (2018) Cellulose hybrid nanocomposites using Napier grass fibers with in situ generated silver nanoparticles as fillers for antibacterial applications. *Int J Biol Macromol* **118**, 99–106.
6. He CR, Kuo YY, Li SY (2017) Lignocellulosic butanol production from Napier grass using semi-simultaneous saccharification fermentation. *Bioresour Technol* **231**, 101–108.
7. Ratsamee S, Akaracharanya A, Leepipatpiboon N, Srinorakutara T, Kitpreechavanich V, Tolieng V (2012) Purple guinea grass: Pretreatment and ethanol fermentation. *Bioresources* **7**, 1891–1906.
8. Patipong T, Lotrakul P, Padungros P, Punnapayak H, Bankeeree W, Prasongsuk S (2019) Enzymatic hydrolysis of tropical weed xylans using xylanase from *Aureobasidium melanogenum* PBUAP46 for xylooligosaccharide production. *3 Biotech* **9**, 56.
9. Takata E, Tsutsumi K, Tsutsumi Y, Tabata K (2013) Production of monosaccharides from Napier grass by hydrothermal process with phosphoric acid. *Bioresour Technol* **143**, 53–58.
10. Wang Y, Cao X, Zhang R, Xiao L, Yuan T-Q, Shi Q, Sun R (2018) Evaluation of xylooligosaccharide production from residual hemicelluloses of dissolving pulp by acid and enzymatic hydrolysis. *RSC Adv* **8**, 35211–35217.
11. Boonchuay P, Techapun C, Seesuriyachan P, Chaiyaso T (2014) Production of xylooligosaccharides from corncob using a crude thermostable endo-xylanase from *Streptomyces thermovulgaris* TISTR1948 and prebiotic properties. *Food Sci Biotechnol* **23**, 1515–1523.
12. Martins M, Ventorim R, Coura R, Maitan-Alfenas G, Alfenas R, Guimaraes V (2018) The β-xylosidase from *Ceratocystis fimbriata* RM35 improves the saccharification of sugarcane bagasse. *Biocatal Agric Biotechnol* **13**, 291–298.
13. Manitchotpisit P, Leathers TD, Peterson SW, Kurtzman CP, Li XL, Eveleigh DE, Lotrakul P, Prasongsuk S, et al (2009) Multilocus phylogenetic analyses, pullulan production and xylanase activity of tropical isolates of *Aureobasidium pullulans*. *Mycol Res* **113**, 1107–1120.
14. Rajewski J, Dobrzyńska-Inger A (2021) Application of response surface methodology (RSM) for the optimization of chromium(III) synergistic extraction by supported liquid membrane. *Membranes* **11**, 854.
15. Bankeeree W, Akada R, Lotrakul P, Punnapayak H, Prasongsuk S (2018) Enzymatic hydrolysis of black liquor xylan by a novel xylose-tolerant, thermostable β-xylosidase from a tropical strain of *Aureobasidium pullulans* CBS 135684. *Appl Biochem Biotechnol* **184**, 919–934.
16. Na Nongkhai S, Piemthongkham P, Bankeeree W, Punnapayak H, Lotrakul P, Prasongsuk S (2023) Xylooligosaccharides produced from sugarcane leaf arabinoxylan using xylanase from *Aureobasidium pullulans* NRRL 58523 and its prebiotic activity toward *Lactobacillus* spp. *Heliyon* **9**, e22107.
17. Peng F, Ren J-L, Xu F, Bian J, Pai P, Sun R-C (2009) Comparative study of hemicelluloses obtained by graded ethanol precipitation from sugarcane bagasse. *J Agric Food Chem* **57**, 6305–6317.
18. Bankeeree W, Lotrakul P, Prasongsuk S, Chaiareekij S, Eveleigh DE, Kim SW, Punnapayak H (2014) Effect of polyols on thermostability of xylanase from a tropical isolate of *Aureobasidium pullulans* and its application in prebleaching of rice straw pulp. *SpringerPlus* **3**, 37.
19. Miller GL (1959) Use of dinitrosalicylic acid reagent for determination of reducing sugar. *Anal Chem* **31**, 426–428.
20. Christov LP, Myburgh J, van Tonder A, Prior BA (1997) Hydrolysis of extracted and fibre-bound xylan with *Aureobasidium pullulans* enzymes. *J Biotechnol* **55**, 21–29.
21. Tuncer M, Ball A (2003) Co-operative actions and degradation analysis of purified xylan-degrading enzymes

from *Thermomonospora fusca* BD25 on oat-spelt xylan. *J Appl Microbiol* **94**, 1030–1035.

22. Ajcharapa C, Sawitree T, Yuwalee U, Keng-Tung W (2019) Green biomass to biogas: A study on anaerobic monodigestion of para grass. *Maejo Int J Energ Environ Comm* **1**, 32–38.
23. Giannoulis KD, Bartzialis D, Skoufogianni E, Gintsioudis I, Danalatos NG (2022) Could a legume-Switchgrass sod-seeding system increase forage productivity? *Plants* **11**, 2970.
24. Phitsuwan P, Charupongrat S, Klednark R, Ratanakhanokchai K (2015) Structural features and enzymatic digestibility of Napier grass fibre treated with aqueous ammonia. *J Ind Eng Chem* **32**, 360–364.
25. Phitsuwan P, Sakka K, Ratanakhanokchai K (2016) Structural changes and enzymatic response of Napier grass (*Pennisetum purpureum*) stem induced by alkaline pretreatment. *Bioresour Technol* **218**, 247–256.
26. Tsai MH, Lee WC, Kuan WC, Sirisansaneeyakul S, Savarajara A (2018) Evaluation of different pretreatments of Napier grass for enzymatic saccharification and ethanol production. *Energy Sci Eng* **6**, 683–692.
27. Stoklosa RJ, Hodge DB (2012) Extraction, recovery, and characterization of hardwood and grass hemicelluloses for integration into biorefining processes. *Ind Eng Chem Res* **51**, 11045–11053.
28. Geng W (2018) Effect of delignification on hemicellulose extraction from switchgrass, poplar, and pine and its effect on enzymatic convertibility of cellulose-rich residues. *Bioresources* **13**, 4946–4963.
29. Xie Y, Guo X, Ma Z, Gong J, Wang H, Lv Y (2020) Efficient extraction and structural characterization of hemicellulose from sugarcane bagasse pith. *Polymers* **12**, 608.
30. Sharma K, Khaire KC, Thakur A, Moholkar VS, Goyal A (2020) Acacia xylan as a substitute for commercially available xylan and its application in the production of xylooligosaccharides. *ACS Omega* **5**, 13729–13738.
31. Peng H, Zhou M, Yu Z, Zhang J, Ruan R, Wan Y, Liu Y (2013) Fractionation and characterization of hemicelluloses from young bamboo (*Phyllostachys pubescens* Mazel) leaves. *Carbohydr Polym* **95**, 262–271.
32. Smith PJ, Wang H-T, York WS, Peña MJ, Urbanowicz BR (2017) Designer biomass for next-generation biorefineries: leveraging recent insights into xylan structure and biosynthesis. *Biotechnol Biofuels* **10**, 286.
33. Tryfona T, Sorieul M, Feijao C, Stott K, Rubtsov DV, Anders N, Dupree P (2019) Development of an oligosaccharide library to characterise the structural variation in glucuronoarabinoxylan in the cell walls of vegetative tissues in grasses. *Biotechnol Biofuels* **12**, 109–128.
34. Duan P, Kaser SJ, Lyczakowski JJ, Phyo P, Tryfona T, Dupree P, Hong M (2021) Xylan structure and dynamics in native *Brachypodium* grass cell walls investigated by solid-state NMR spectroscopy. *ACS Omega* **6**, 15460–15471.
35. Guido ES, Silveira J, Kalil SJ (2019) Enzymatic production of xylooligosaccharides from beechwood xylan: effect of xylanase preparation on carbohydrate profile of the hydrolysates. *Int Food Res J* **26**, 713–721.
36. Lopes AM, Ferreira Filho EX, Moreira LRS (2018) An update on enzymatic cocktails for lignocellulose breakdown. *J Appl Microbiol* **125**, 632–645.
37. Akobi C, Hafez H, Nakhla G (2017) Impact of furfural on biological hydrogen production kinetics from synthetic lignocellulosic hydrolysate using mesophilic and thermophilic mixed cultures. *Int J Hydrog Energy* **42**, 12157–12172.
38. Suwannarangsee S, Arnthong J, Eurwilaichitr L, Champreda V (2014) Production and characterization of multi-polysaccharide degrading enzymes from *Aspergillus aculeatus* BCC199 for saccharification of agricultural residues. *J Microbiol Biotechnol* **24**, 1427–1437.
39. Wang F, Yao Z, Zhang X, Han Z, Chu X, Ge X, Lu F, Liu Y (2022) High-level production of xylose from agricultural wastes using GH11 endo-xylanase and GH43 β-xylosidase from *Bacillus* sp. *Bioprocess Biosyst Eng* **45**, 1705–1717.

Appendix A. Supplementary data

Table S1 Biomass composition of grass samples.

Grass sample	Biomass composition (% (w/w))[a]				
	Cellulose	Hemicellulose	Lignin	Ash	Other
NG	31.3 ± 1.5	33.7 ± 0.6	8.7 ± 0.6	3.0 ± 0.6	23.3 ± 1.2
PG	33.8 ± 0.6	27.7 ± 0.6	6.0 ± 0.8	2.7 ± 0.5	29.7 ± 0.4

[a] Mean ± SD derived from three replicates.

Table S2 BBD-RSM used for optimization of xylan extraction from NG and PG.

Run	Actual level			Relative xylan recovery (% of hemicellulose content)			
	NaOH concentration	Steaming time	Liquid-to-solid ratio	NG		PG	
	(X_1; % w/v)	(X_2; min)	(X_3; ml/g biomass)	Observed[a]	Predicted	Observed[a]	Predicted
1	12 (−1)	30 (−1)	10 (0)	63.7 ± 4.3	64.8	73.4 ± 2.8	79.3
2	18 (+1)	30 (−1)	10 (0)	78.4 ± 9.0	78.0	96.3 ± 3.3	91.4
3	12 (−1)	60 (+1)	10 (0)	63.6 ± 1.2	64.1	77.6 ± 6.5	82.4
4	18 (+1)	60 (+1)	10 (0)	64.9 ± 3.1	64.1	99.9 ± 6.2	94.2
5	12 (−1)	45 (0)	5 (−1)	8.9 ± 0.9	6.9	31.3 ± 1.0	21.1
6	18 (+1)	45 (0)	5 (−1)	7.4 ± 0.5	7.6	44.3 ± 3.2	44.3
7	12 (−1)	45 (0)	15 (+1)	76.2 ± 2.3	76.8	95.7 ± 3.2	96.3
8	18 (+1)	45 (0)	15 (+1)	87.6 ± 3.0	89.9	86.2 ± 3.0	97.7
9	15 (0)	30 (−1)	5 (−1)	11.4 ± 2.3	12.4	21.5 ± 1.8	25.3
10	15 (0)	60 (+1)	5 (−1)	7.4 ± 0.5	9.0	28.8 ± 2.0	33.4
11	15 (0)	30 (−1)	15 (+1)	94.4 ± 3.7	93.4	99.1 ± 7.2	93.8
12	15 (0)	60 (+1)	15 (+1)	82.0 ± 2.0	82.5	96.4 ± 4.3	91.9
13	15 (0)	45 (0)	10 (0)	74.5 ± 3.8	76.0	89.7 ± 1.0	92.8
14	15 (0)	45(0)	10 (0)	76.2 ± 9.7	76.0	95.1 ± 7.3	92.8
15	15 (0)	45 (0)	10 (0)	73.1 ± 2.3	76.0	93.6 ± 4.4	92.8

[a] Mean ± SD derived from three replicates.

Table S3 ANOVA for response surface quadratic model of xylan extraction from NG.

Source	Sum of squares	Mean square	F-value	p-value	
Model	14156.6	1573.0	341.2	< 0.0001	Significant
X_1-NaOH concentration	83.2	83.2	18.1	0.008	
X_2-Steaming time	112.7	112.7	24.5	0.004	
X_3-Liquid-to-solid ratio	11643.0	11643.0	2525.9	< 0.0001	
X_1X_2	45.4	45.4	9.9	0.03	
X_1X_3	41.4	41.4	9.0	0.03	
X_2X_3	17.5	17.5	3.8	0.11	
X_1^2	105.8	105.8	23.0	0.01	
X_2^2	9.5	9.53	2.1	0.21	
X_3^2	2167.2	2167.2	470.2	< 0.0001	
Residual	23.2	4.6			
Lack of fit	18.3	6.1	2.54	0.3	Not significant
Pure error	4.8	2.4			
Cor Total	14179.7				

Relative xylan recovery: $R^2 = 0.99$, R^2 (adjacent) = 0.99, CV = 3.7%.

Table S4 ANOVA for response surface quadratic model of xylan extraction from PG.

Source	Sum of squares	Mean square	F-value	p-value	
Model	11067.3	1229.7	14.6	0.004	Significant
X_1-NaOH concentration	295.1	295.1	3.5	0.12	
X_2-Steaming time	18.9	18.9	0.2	0.66	
X_3-Liquid-to-solid ratio	7909.9	7910.0	93.6	0.0002	
X_1X_2	0.1	0.1	0.001	0.97	
X_1X_3	125.8	125.8	1.5	0.28	
X_2X_3	24.8	24.8	0.3	0.61	
X_1^2	8.8	8.8	0.1	0.76	
X_2^2	73.3	73.3	0.9	0.39	
X_3^2	2669.7	2669.7	31.6	0.003	
Residual	422.6	84.5			
Lack of fit	406.8	135.6	17.2	0.06	Not significant
Pure error	15.8	7.9			
Cor Total	11489.9				

Relative xylan recovery: $R^2 = 0.96$, R^2 (adjacent) $= 0.90$, CV $= 12.2\%$.

Table S5 Sugar composition of NGX and PGX.

Extracted xylan	Sugar composition (%)*		
	Xylose	Arabinose	Glucuronic acid
NGX	77.2 ± 0.7	20.6 ± 0.4	2.2 ± 0.8
PGX	76.7 ± 0.3	20.9 ± 0.4	2.4 ± 0.1

* Data were presented as the average value ± standard deviation.

Table S6 CCD-RSM used for optimization of XOs production from NGX and PGX.

Run	Actual level		The amount of reducing sugars (mg/g xylan)			
	Endoxylanase dosage	Incubation time	NGX		PGX	
	(A_1; U/g initial xylan)	(A_2; h)	Observed[a]	Predicted	Observed[a]	Predicted
1	25 (−1)	24 (−1)	95.7 ± 3.0	99.2	94.9 ± 2.9	95.2
2	75 (+1)	24 (−1)	148.9 ± 9.9	152.0	148.9 ± 13.5	148.2
3	25 (−1)	72 (+1)	125.5 ± 7.6	131.5	125.7 ± 2.3	124.9
4	75 (+1)	72 (+1)	162.5 ± 3.2	168.2	172.9 ± 8.08	171.2
5	15 (−1.414)	48 (0)	107.1 ± 1.5	103.0	96.3 ± 7.0	97.17
6	85 (+1.414)	48 (0)	169.8 ± 4.9	165.6	165.2 ± 2.3	166.7
7	50 (0)	14 (−1.414)	127.1 ± 3.1	124.3	119.6 ± 1.6	119.6
8	50 (0)	82 (+1.414)	165.0 ± 9.6	158.6	155.6 ± 6.3	157.0
9	50 (0)	48 (0)	149.7 ± 5.8	153.6	155.2 ± 3.8	155.3
10	50 (0)	48 (0)	158.4 ± 9.3	153.6	156.0 ± 1.9	155.3
11	50 (0)	48 (0)	152.7 ± 4.0	153.6	154.6 ± 5.3	155.3

[a] Mean ± SD derived from three replicates.

Table S7 ANOVA for response surface quadratic model of XOs production from NGX.

Source	Sum of squares	Mean square	F-value	p-value	
Model	5851.4	1170.3	26.7	0.001	Significant
A_1-Endoxylanase dosage	4001.7	4001.7	91.4	0.0002	
A_2-Incubation time	1174.8	1174.8	26.8	0.004	
A_1A_2	64.7	64.7	1.5	0.28	
A_1^2	547.6	547.6	12.5	0.02	
A_2^2	208.7	208.7	4.8	0.08	
Residual	218.9	43.8			
Lack of fit	179.4	59.8	3.0	0.26	Not significant
Pure error	39.5	19.8			
Cor Total	6070.3				

The amount of reducing sugars: $R^2 = 0.96$, R^2 (adjacent) $= 0.93$, CV $= 4.1\%$.

Table S8 ANOVA for response surface quadratic model of XOs production from PGX.

Source	Sum of squares	Mean square	F-value	p-value	
Model	7286.3	1457.3	831.4	< 0.0001	Significant
A_1-Endoxylanase dosage	4928.2	4928.2	2811.8	< 0.0001	
A_2-Incubation time	1394.3	1394.3	795.5	< 0.0001	
A_1A_2	11.3	11.3	6.4	0.05	
A_1^2	800.0	800.1	456.5	< 0.0001	
A_2^2	404.8	404.8	230.9	< 0.0001	
Residual	8.8	1.8			
Lack of fit	7.7	2.6	5.0	0.17	Not significant
Pure error	1.0	0.5			
Cor Total	7295.1				

The amount of reducing sugars: $R^2 = 0.99$, R^2 (adjacent) $= 0.99$, CV $= 0.9\%$.

Table S9 BBD -RSM used for optimization of xylose production from NGX and PGX.

Run	Actual level			Xylose yield (mg/g xylan)			
	Endoxylanase dosage	β-xylosidase dosage	Incubation time	NGX		PGX	
	(B_1; U/g xylan)	(B_2; U/g xylan)	(B_3; h)	Observed[a]	Predicted	Observed[a]	Predicted
1	30 (−1)	30 (−1)	12 (0)	119.7 ± 4.4	117.8	126.8 ± 1.6	134.8
2	70 (+1)	30 (−1)	12 (0)	135.5 ± 2.8	133.9	150.2 ± 6.4	145.7
3	30 (−1)	70 (+1)	12 (0)	128.8 ± 1.3	130.4	136.6 ± 2.0	141.2
4	70 (+1)	70 (+1)	12 (0)	141.7 ± 1.8	143.7	182.9 ± 3.9	174.9
5	30 (−1)	50 (0)	6 (−1)	105.1 ± 1.2	104.4	123.3 ± 0.9	118.9
6	70 (+1)	50 (0)	6 (−1)	124.4 ± 2.2	123.3	129.4 ± 4.1	137.5
7	30 (−1)	50 (0)	18 (+1)	131.4 ± 0.8	132.5	149.1 ± 2.5	141.0
8	70 (+1)	50 (0)	18 (+1)	142.3 ± 0.8	143.0	162.5 ± 3.0	166.9
9	50 (0)	30 (−1)	6 (−1)	100.6 ± 0.8	103.3	108.7 ± 2.2	105.1
10	50 (0)	70 (+1)	6 (−1)	121.7 ± 0.9	120.8	126.4 ± 1.7	126.3
11	50 (0)	30 (−1)	18 (+1)	132.7 ± 1.0	133.6	134.0 ± 0.7	134.1
12	50 (0)	70 (+1)	18 (+1)	141.1 ± 0.4	138.5	145.2 ± 0.6	148.7
13	50 (0)	50 (0)	12 (0)	132.6 ± 1.2	130.2	135.2 ± 0.1	132.0
14	50 (0)	50 (0)	12 (0)	129.1 ± 0.4	130.2	130.1 ± 0.1	132.0
15	50 (0)	50 (0)	12 (0)	128.8 ± 0.75	130.2	130.7 ± 0.3	132.0

[a] Mean ± SD derived from three replicates.

Table S10 ANOVA for response surface quadratic model of xylose production from NGX.

Source	Sum of squares	Mean square	F-value	p-value	
Model	2030.0	225.6	27.59	0.001	Significant
B_1-Endoxylanase dosage	432.7	432.7	52.92	0.001	
B_2-β-xylosidase dosage	251.0	251.0	30.70	0.003	
B_3-Incubation time	1145.4	1145.4	140.1	< 0.0001	
B_1B_2	2.0	2.0	0.25	0.64	
B_1B_3	17.8	17.8	2.2	0.20	
B_2B_3	39.9	39.9	4.9	0.08	
B_1^2	8.4	8.4	1.0	0.36	
B_2^2	0.21	0.2	0.03	0.88	
B_3^2	127.0	127.0	15.5	0.01	
Residual	40.9	8.2			
Lack of fit	32.0	10.7	2.4	0.31	Not significant
Pure error	8.9	4.4			
Cor Total	2070.9				

Xylose yield: $R^2 = 0.98$, R^2 (adjacent) $= 0.94$, CV $= 2.2\%$.

Table S11 ANOVA for response surface quadratic model of xylose production from PGX.

Source	Sum of squares	Mean square	F-value	p-value	
Model	4111.0	456.8	6.0	0.03	Significant
B_1-Endoxylanase dosage	995.3	995.3	13.1	0.02	
B_2-β-xylosidase dosage	639.3	639.3	8.4	0.03	
B_3-Incubation time	1324.3	1324.3	17.5	0.01	
B_1B_2	130.7	130.7	1.7	0.25	
B_1B_3	13.3	13.3	0.18	0.69	
B_2B_3	10.7	10.7	0.14	0.72	
B_1^2	811.2	811.2	10.7	0.02	
B_2^2	19.9	19.9	0.26	0.63	
B_3^2	121.6	121.6	1.6	0.26	
Residual	379.4	75.9			
Lack of fit	363.9	121.3	15.6	0.06	Not significant
Pure error	15.5	7.8			
Cor Total	4490.4				

Xylose yield: $R^2 = 0.91$, R^2 (adjacent) $= 0.76$, CV $= 6.3\%$.

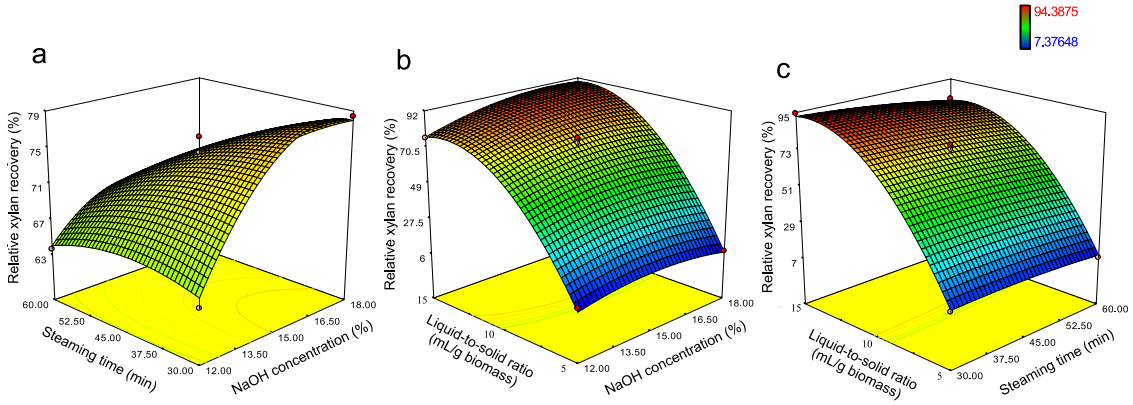

Fig. S1 Response surface plot for optimal condition of the relative xylan recovery from NG: (a) Effect of NaOH concentration and steaming time, (b) Effect of NaOH concentration and liquid-to-solid ratio, and (c) Effect of steaming time and liquid-to-solid ratio.

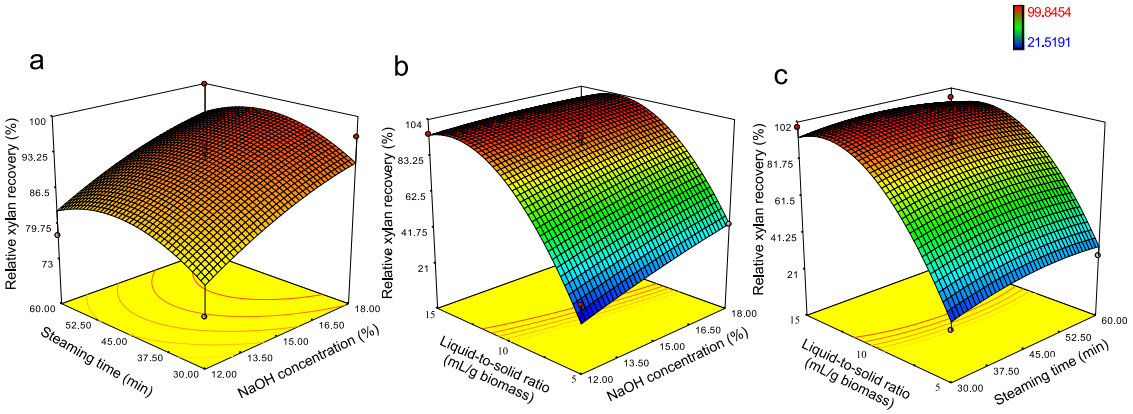

Fig. S2 Response surface plot for optimal condition of the relative xylan recovery from PG: (a) Effect of NaOH concentration and steaming time, (b) Effect of NaOH concentration and liquid-to-solid ratio, and (c) Effect of steaming time and liquid-to-solid ratio.

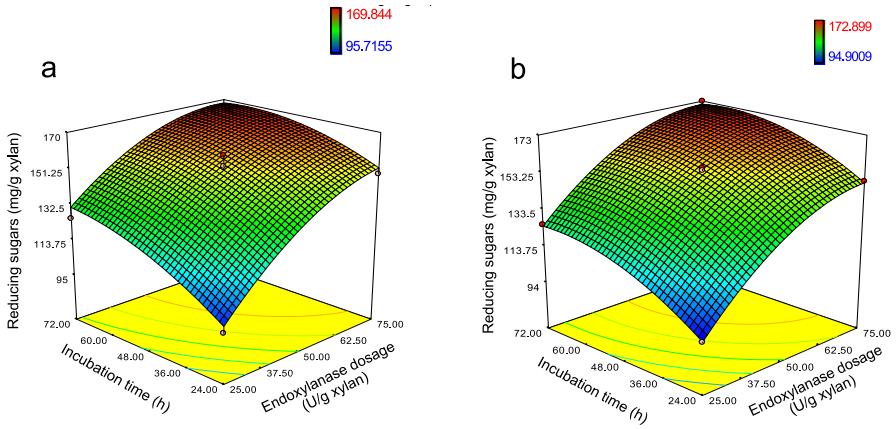

Fig. S3 Response surface plots for optimal condition of partial enzymatic hydrolysis of (a) NGX and (b) PGX for determination of the releasing of reducing sugars.

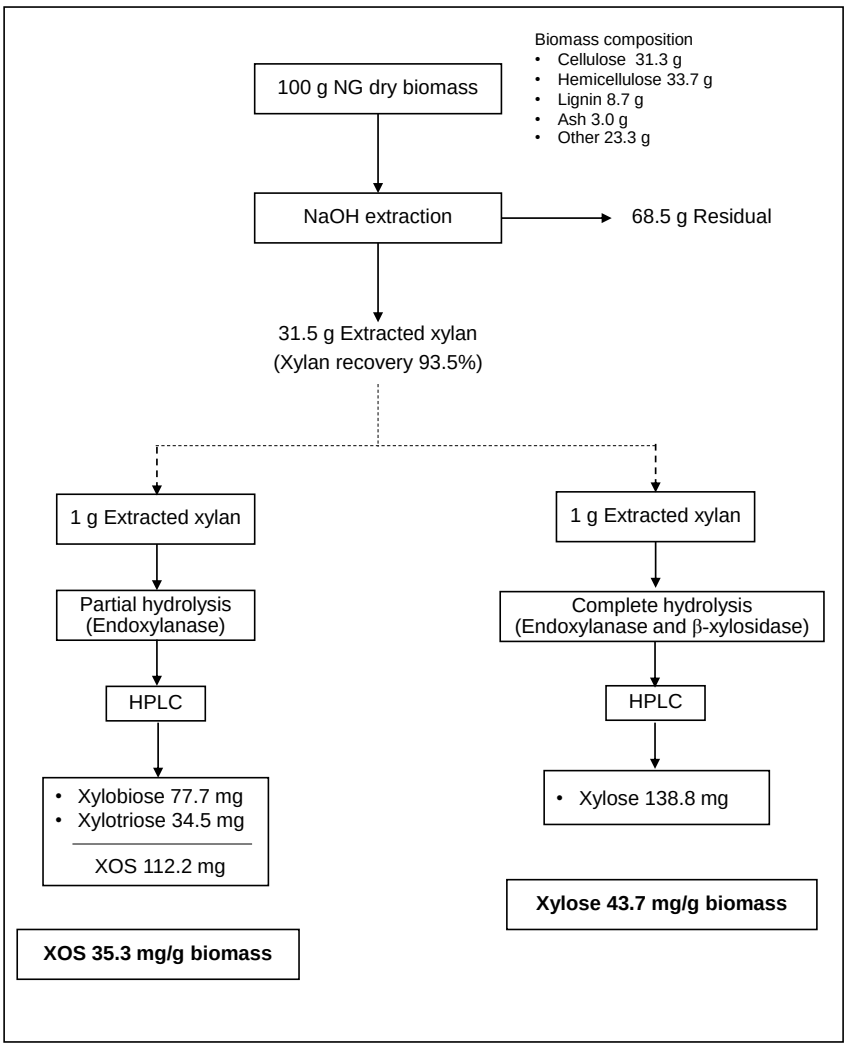

Fig. S4 The mass balance to produce XOs and xylose from NGX.

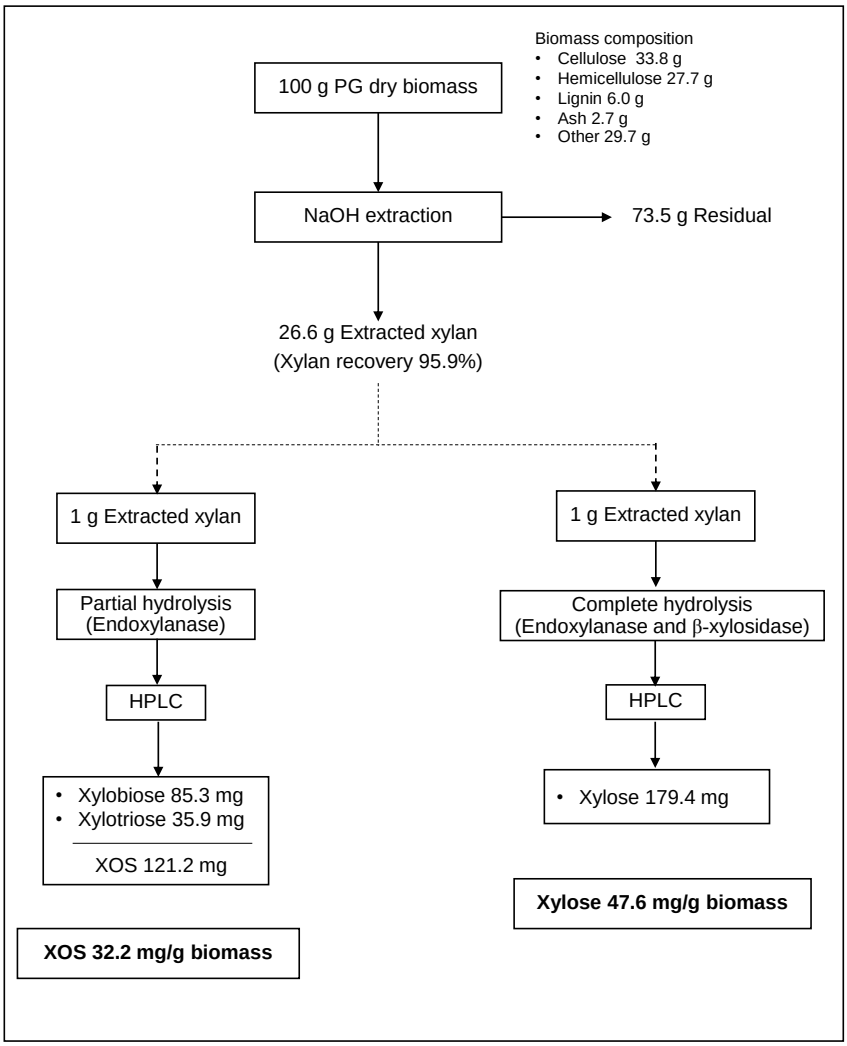

Fig. S5 The mass balance to produce XOs and xylose from PGX.

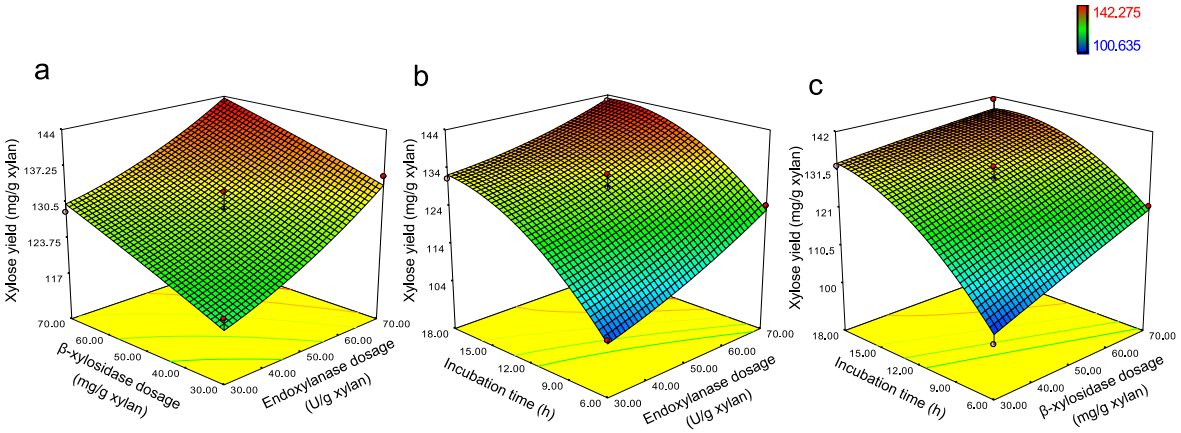

Fig. S6 Response surface plots for optimal condition of xylose production from NGX: (a) Effect of β-xylosidase and endoxylanase dosages, (b) Effect of incubation time and endoxylanase dosage, and (c) Effect of incubation time and β-xylosidase dosage.

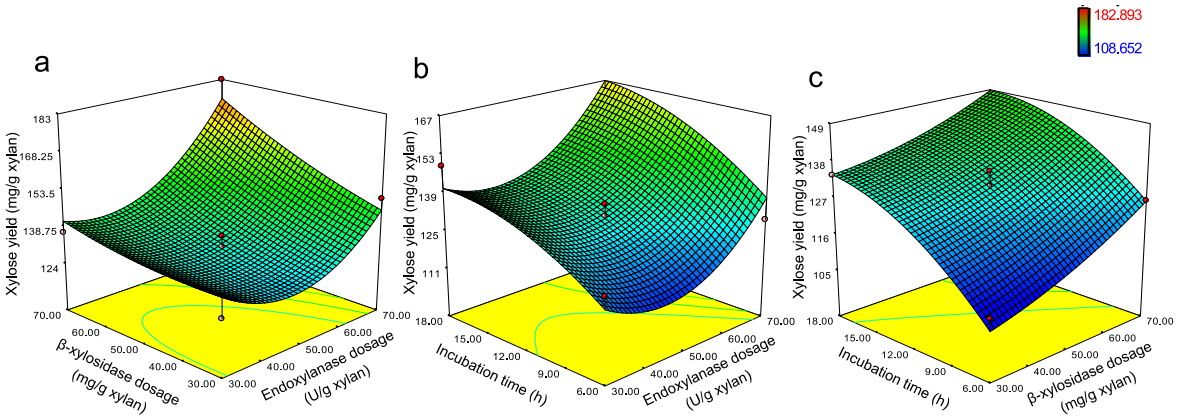

Fig. S7 Response surface plots for optimal condition of xylose production from PGX: (a) Effect of β-xylosidase and endoxylanase dosages, (b) Effect of incubation time and endoxylanase dosage, and (c) Effect of incubation time and β-xylosidase dosage.

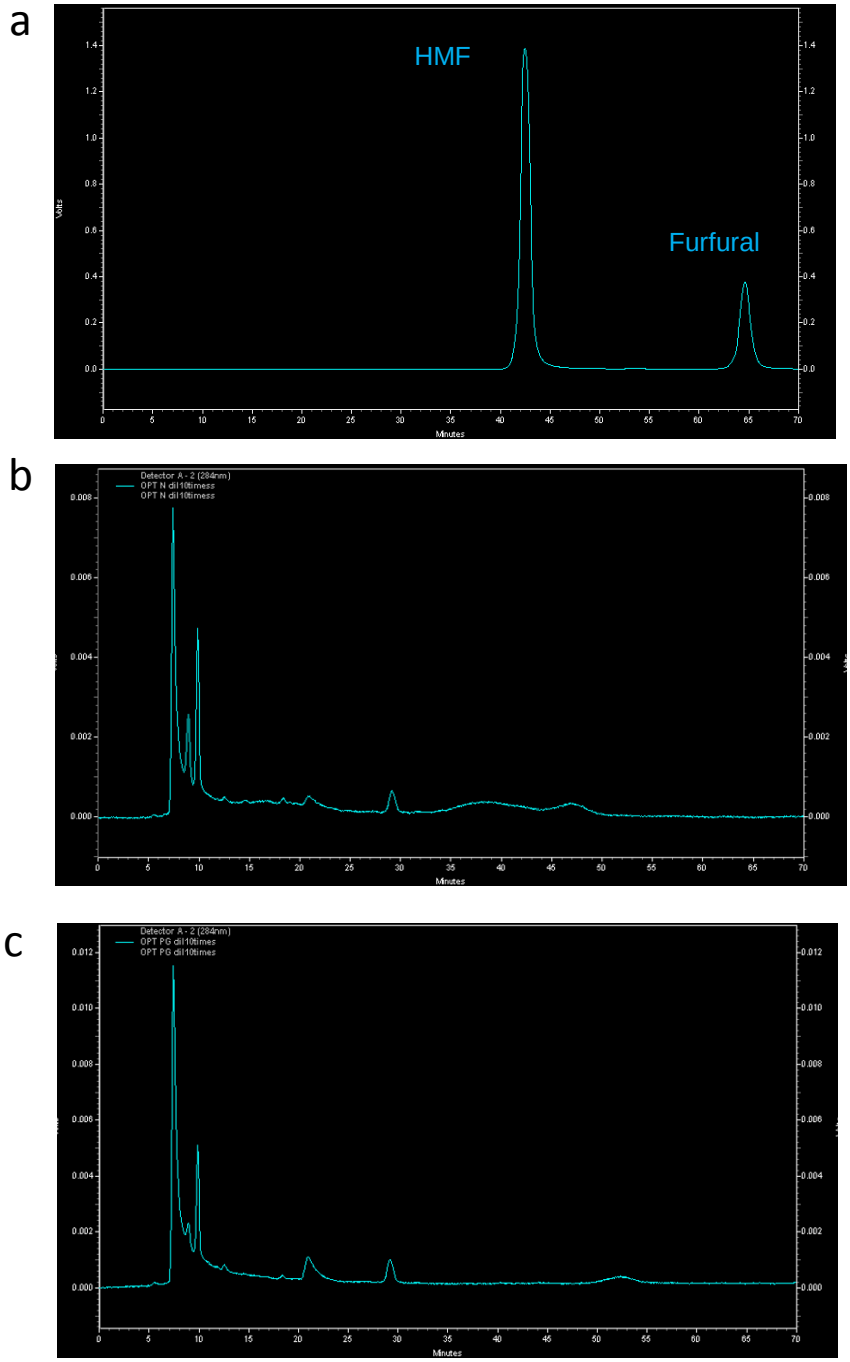

Fig. S8 HPLC chromatograms: (a) standard of furfural and hydroxymethylfurfural (HMF), (b) NGX hydrolysate, and (c) PGX hydrolysate.